Computation by symmetry operations in a structured model of the brain: Recognition of rotational invariance and time reversal

John V. McGrann,* Gordon L. Shaw, Krishna V. Shenoy,† Xiaodan Leng,‡ and Robert B. Mathews§
Center for the Neurobiology of Learning and Memory and Department of Physics, University of California, Irvine, California 92717
(Received 24 September 1993)

Symmetries have long been recognized as a vital component of physical and biological systems. What we propose here is that symmetry operations are an important feature of higher brain function and result from the spatial and temporal modularity of the cortex. These symmetry operations arise naturally in the trion model of the cortex. The trion model is a highly structured mathematical realization of the Mountcastle organizational principle [Mountcastle, in *The Mindful Brain* (MIT, Cambridge, 1978)] in which the cortical column is the basic neural network of the cortex and is comprised of subunit minicolumns, which are idealized as trions with three levels of firing. A columnar network of a small number of trions has a large repertoire of quasistable, periodic spatial-temporal firing magic patterns (MP's), which can be excited. The MP's are related by specific symmetries: Spatial rotation, parity, "spin" reversal, and time reversal as well as other "global" symmetry operations in this abstract internal language of the brain. These MP's can be readily enhanced (as well as inherent categories of MP's) by only a small change in connection strengths via a Hebb learning rule. Learning introduces small breaking of the symmetries in the connectivities which enables a symmetry in the patterns to be recognized in the Monte Carlo evolution of the MP's. Examples of the recognition of rotational invariance and of a time-reversed pattern are presented. We propose the possibility of building a logic device from the hardware implementation of a higher level architecture of trion cortical columns.

PACS number(s): 87.10.+e

I. INTRODUCTION

Symmetries have long been recognized as a vital component of physical and biological systems [1]. It is apparent that as neuroanatomical and neurophysiological techniques have improved in the past decade, more and more structure has been found in the cortex. We expect this trend to continue. We propose here that symmetry operations performed by the brain are an important feature of higher brain function and result from this spatial and temporal structure of the cortex [2]. This modular structure with symmetry among the connections introduces symmetries among the "inherent" spatial-temporal firing patterns in the cortex. The symmetries of these inherent firing patterns can then be "exploited" to perform higher level computations or symmetry operations. Learning (through a Hebb rule [3]) introduces small breaking of the symmetries in the connectivities which enables a symmetry in the patterns to be recognized in the Monte Carlo evolution of the patterns. This technique of computation by symmetry operators may play an important role in mammalian higher brain function. Using the trion model of the cortex [4–7], we will present specific, simple examples of this in the recognization of rotational invariance and in the recognition of a time-reversed pattern.

Mountcastle [8] proposed that the cortical column [2] is the basic network in the cortex and is comprised of small irreducible processing units called minicolumns. A very simple pinwheel representation [9] of the minicolumns in the visual cortex [2,8] had been suggested. Recently the optical recording results by Bonhoefer and Grinvald [2] not only show a strong similarity to these representations but find both helicities in the representation of the orientation minicolumns. We display this in a very highly idealized, structured, and generalized scheme in Fig. 1. The column has the capability of being excited into complex spatial-temporal firing patterns. The assumption is that higher mammalian processes involve the creation and transformation of such complex spatial-temporal firing patterns (in contrast to a "code" which involves sets of neurons firing with high frequency). Evidence [2,10] is accumulating in support of the viability of Mountcastle spatial-temporal code [8] for the "internal language" of the cortex.

The trion model of the cortical column, summarized in Sec. II, is a mathematical realization of Mountcastle's organizational principle. It was developed starting from Little's [11] neural network analogy to the Ising spin system, and modified in a direction inspired by the ANNNI (axial next-nearest neighbor Ising) model results of Fisher

*Present address: Westinghouse Corporation, Electronics Systems Group, Baltimore, MD 21203.
†Present address: Department of Electrical Engineering and Computer Science, Massachusetts Institute of Technology, Cambridge, MA 02139.
‡Also at: Department of Applied Mathematics, University of Montreal, Montreal, Canada.
§Present address: Department of Physics, California Poly State University, San Luis Obispo, CA 94307.

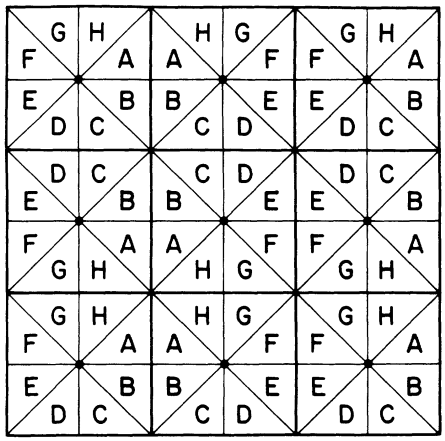

FIG. 1. Highly schematic representation of the Mountcastle [8] principle of cortical organization. Each square, following [9], represents a cortical column (horizontal dimension roughly 700 μm, see Fig. 14, comprising the six vertical layers of dimension roughly 2000 μm) while each triangle is a minicolumn which encodes the relevant parameter in the stimuli such as line orientation in the visual cortex [2] shown here by capital letters. We note that the optical recording results by Bonhoeffer and Grinvald [2] in secondary visual cortex show a strong similarity to the cartoon idealized primary visual cortex shown here.

and Selke [12]. A trion, Fig. 2, represents an idealized minicolumn or roughly 100 neurons, and has three levels of firing activity, above average, average, and below average. A column with a small number of trions having structured connections yields a large repertoire of quasistable, periodic spatial-temporal firing patterns, defined as magic patterns or MP's which can be excited. These inherent patterns are called magic patterns or MP's because of their ability to be learned or enhanced via a Hebb learning rule to a large cycling probability. The repertoire of (periodic) MP's is found by evolving all possible initial states (of the first two time steps) by following the most probable or deterministic path. The

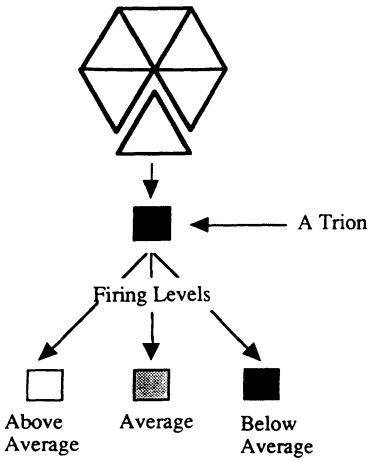

FIG. 2. We identify a minicolumn with the idealized trion and the basic network of trions is the cortical column. As shown, the trion has three levels of firing activity.

symmetries relating the MP's in a repertoire are discussed in Sec. III. In a full probabilistic (or Monte Carlo) evolution, the MP's evolve in natural sequences from one to another. The probability of each MP remaining in that pattern can be enhanced by even a small change in connection strengths using a Hebbian learning rule [3,13–15].

One of the important and well-studied problems in visual pattern recognition is to understand the nature of how the brain recognizes rotated objects [16]. If one sees a rotated form of a familiar object, the recognition time will depend linearly on the angle or rotation. These properties are not readily incorporated into standard neural networks [17]. In this paper, we show that this recognition of rotational invariance is built into the highly structured trion model of cortical organization due to its natural symmetry relations. The symmetry of the connections among the trions introduces sets of MP's related by symmetry operations, in particular, spatial rotations. Other symmetries relating MP's in a repertoire of the trion model include parity, spin reversal, and time reversal. Each MP can be learned (or selected out) through a correlated Hebbian rule with small changes in connectivity, which can break the symmetry. As a result, the probability of the learned MP for remaining excited is increased and its basin of attraction for recall is enlarged. Consider a simplified example in which a specific visual object (VO) is represented in the cortex by one of the MP's. Spatially rotated VO's are represented by spatial rotations of the MP corresponding to the standing VO. The VO seen in a normal standing position is learned with the Hebb rule and the symmetry among the connections is broken by a small amount. This learning occurs as a natural consequence of repeated presentation of the standing VO. When a rotated VO is seen, the rotated VO MP is excited in the cortex, and evolves in a Monte Carlo calculation into the MP for the standing VO, thereby identifying it as related to the VO; the number of time steps to evolve is linearly related to the amount of rotation. This example is presented in Sec. IV. A second example is presented in Sec. IV showing the recognition of time-reversed MP's (as well as spatially rotated ones), again through the Monte Carlo evolutions once the symmetry in the connectivities is broken by a small amount through learning.

Consider these symmetry operations in the dynamics of the cortical column above to be the basic elements of higher brain function. Based on this, we generalize our results and speculate, in the discussion Sec. V, on the possibility of building a logic device from the hardware implementation of a higher level architecture, Fig. 1, of trion cortical columns.

II. SUMMARY OF TRION MODEL OF THE CORTICAL COLUMN

The trion model [4–7] represents a mathematical realization of Mountcastle's [8] columnar organizational principle of cortex. The interactions among the trions are taken to be localized, competing (between excitation and inhibition), and highly structured, and the firing state of

the network (cortical column) of the distinguishable trions at time $n\tau$ is updated in a probabilistic way related to the states of the two previous discrete time steps $(n-1)\tau$ and $(n-2)\tau$ as in Fig. 3. We expect these time steps τ to be roughly 25–100 ms. The probability $P(S_i)$ of the ith trion having a firing level or state S_i at time $n\tau$ is given by

$$P(S_i)=\frac{g(S_i)\exp[BM_iS_i]}{\sum_S g(S)\exp[BM_iS]}\ ,$$
$$M_i=\sum_j [V_{ij}S_j'+W_{ij}S_j'']-V_i\ , \tag{1}$$

where S_j' and S_j'' are the states of the jth trion at the two earlier times $(n-1)\tau$ and $(-n2)\tau$, respectively. V_{ij} and W_{ij} are the interactions between trions i and j at time $n\tau$ from times $(n-1)\tau$ and $(n-2)\tau$, respectively; V_i is an effective firing threshold. The three possible firing states (of each trion) denoted by $+,0,-$ for $S=1,0,-1$ represent, respectively, a large "burst" of firing, an average burst, and a below average firing (see Fig. 2). The term $g(S)$ with $g(0)\gg g(\pm)$ takes into account the number of equivalent firing configurations of the trion's internal neuronal constituents [18]. [For example, in a trion representing a group of 90 neurons, firing levels of $+,0,-$ could correspond to 90–61, 60–31, 30–0 neurons firing, respectively. There are many more equivalent combinatorial ways of generating the 60–31 level from the indistinguishable neurons. This feature, $g(0)\gg g(+)=g(-)$, gives stability to the trion model firing patterns.] The fluctuation parameter B is inversely proportional to the noise and results [19] from the statistical nature of neurotransmitter release from the synapses [20]. Studies of the trion model for learning and memory and higher brain function have been reported. Basically, the success of these studies is due to the fact that the localized, competing (between excitation and inhibition) interactions with high symmetry yield a huge repertoire of inherent quasistable, periodic firing patterns, MP's, any of which can be readily learned or enhanced with only small changes in the interaction strengths using the Hebb learning algorithm

$$\Delta V_{ij}=\varepsilon\sum_n^{\text{pattern}} S_i(n\tau)S_j((n-1)\tau)\ ,$$
$$\Delta W_{ij}=\varepsilon\sum_n^{\text{pattern}} S_i(n\tau)S_j((n-2)\tau)\ , \qquad \varepsilon>0 \tag{2}$$

which allows for both increases and decreases of interaction strengths. (Simply extending this learning rule to a third time step using the correlation [14,15]

$$\sum S_i(n\tau)S_j((n-3)\tau)$$

significantly enhances the effects of learning with a smaller change in the total connectivity.) Let us define the cycling probability P_C (MP) that the firing pattern for the columnar trion network remains in the MP for one cycle of the repeating MP. The P_C(MP) is calculated by multiplying the probabilities $P(S_i)$, Eq. (1), of each trion i being in the state S at time $n\tau$, given by that MP for its whole cycle length:

$$P_C(\text{MP})=\prod_n\prod_i P(S_i(n\tau))\ . \tag{3}$$

Then as a result of learning a MP using the Hebb [4] algorithm (2), the cycling probability P_C(MP), (3), is increased. Further, after learning, many more initial states will go to the learned MP (and some related MP's). Note that these MP's evolve in natural sequences from one to another in a probabilistic Monte Carlo calculation.

It was shown in [6] that there exist a series of phase transitions at precise values $B(n)$ giving new repertoires of firing patterns: Rewriting the statistical factors $g(S)/g(0)=\exp(-u^2S^2)$, then (1) becomes

$$P(S_i)\propto\exp\left[-u^2S_i^2+BS_i\left[\sum_j (W_{ij}S_j''+V_{ij}S_j')-V_i\right]\right]\ . \tag{4}$$

The cancellation of the u^2 and B terms in the exponential allow the $S_i=0$ level to compete with the 1 and -1 firing levels. There then exist a series of "transition temperatures B^{-1}"

$$B(n)=u^2/n \tag{5}$$

for specific integers n related to the V's and W's. These $B(n)$ separate regions with different logic and thus different repertoires of MP's.

The simulations of a trion columnar network are simply performed.

(1) We specify the parameters of the trion network: the number of trions N, the degeneracy factors $g(S_i)$, the connectivities V_{ij} and W_{ij}, the firing thresholds V_i, and the fluctuation parameter B.

(2) A choice for the firing states for the initial two time steps is made. Since each of the N trions in each time step has three possible firing levels S, there are 3^{2N} possible initial choices.

(3) Given the firing states for each trion at the two earlier times $(n-1)\tau$ and $(n-2)\tau$, the probability $P(S_i)$ for

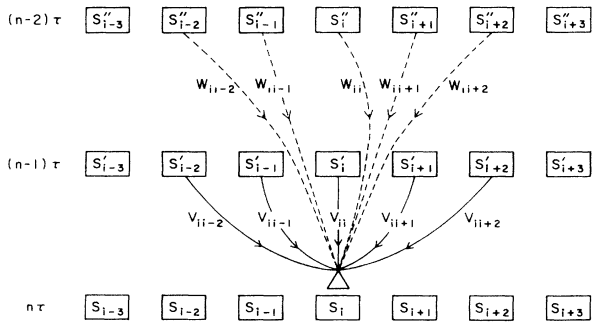

FIG. 3. One network of trions at three time steps, showing the firing states S and the connections V and W, see Eq. (1). For N trions in the columnar network, we have the ringlike connections trion i = trion $i+N$ as in Fig. 2.

the ith trion being in state S_i at time $n\tau$ is calculated from Eq. (1).

Having made the choice of parameter (1) above, the repertoire of MP's or inherent, quasistable, periodic firing patterns is found as follows. For a given initial firing state (2), follow the procedure of always choosing the S for each trion which has the largest probability (1) or most probable path, i.e., the largest exponent in (4) for $P(S)$. Then the time evolution rapidly goes into a repeating spatial-temporal pattern or MP. Define the operator Γ which temporally evolves a MP according to its most probable path for its cycle length N_c. Then a MP is an eigenfunction of Γ with eigenvalue 1:

$$\Gamma(\mathrm{MP})=(\mathrm{MP})\ . \tag{6}$$

An explicit representation of Γ can be written down from (1) or (4). Going through all possible initial states (2) gives all the MP's (the repertoire of MP's) as well as the number of initial states recalling each MP and the average time to recall a MP. (See Fig. 4 below for an explicit example of a repertoire of MP's.) A MP has the property of being readily learned or enhanced using the Hebb learning rule in Eq. (2) with only a relatively small change in the connections V and W. After learning, more initial states will go to the learned MP (and some related MP's) and the cycling probability $P_C(\mathrm{MP})$, Eq. (3) will be increased. Furthermore, an arbitrary spatial-temporal pattern cannot be readily learned. Only a MP can be learned in a selective manner.

III. SYMMETRIES OF THE MP's IN A REPERTOIRE

Consider a symmetry operator α acting on (6): $\alpha\Gamma(\mathrm{MP})=\alpha(\mathrm{MP})$. Then if α commutes with Γ, $\alpha(\mathrm{MP})$ is also a MP:

$$\alpha\Gamma(\mathrm{MP})=\alpha\Gamma\alpha^{-1}\alpha(\mathrm{MP})=\Gamma\alpha(\mathrm{MP})=\alpha(\mathrm{MP})$$
$$\text{for } \alpha\Gamma\alpha^{-1}=\Gamma\ . \tag{7}$$

Thus we expect for our structured connectivity in the trion model that there will be a number of symmetries α that will be useful to use to characterize a repertoire of MP's. To be explicit, let us examine a specific example of the repertoire of MP's for structured connections in an $N=6$ network. Consider the connectivities and other parameters in Eq. (1) to be as follows:

$$V_{ii}=2,\quad V_{i,i+1}=V_{i,i-1}=1,\quad W_{ij}=-V_{ij}\ , \tag{8}$$

thresholds $V_i=0$, all other V_{ij} equal to $0, g(0)/g(\pm)=500$ or $u^2=6.215$, and B above the first transition $B(1)=6.215$ in (5). Then following the calculations in Sec. II above, each of the $3^{12}=531\,441$ possible choices for the initial states is followed to find the 155 MP's shown in Fig. 4. These 155 MP's can be placed into 34 sets where the MP's in a set are related to each other by a spatial rotation among trions, R, among the (distinguishable) trions. It is evident from (8) and our ring boundary conditions that $\alpha=R$ commutes with Γ. Other symmetries among these MP's can be used to categorize groups of MP's. We see that a parity reflection P, a time-reversal operation T, and the combination PT will relate different MP's as shown in Fig. 5. That T commutes with Γ is not obvious. In Fig. 4, the 34 sets of MP's are placed in 20 groups with MP's in each group related by the symmetry operations α equal to P, T, and PT (Fig. 5) in addition to rotation R.

An additional symmetry operator changes firing level "spin" S to $-S$. In analogy with physical systems, let us define this as C, the "charge" conjugation operator. An example of a repertoire in which distinct MP's are related by C is seen in Table 5 of [5].

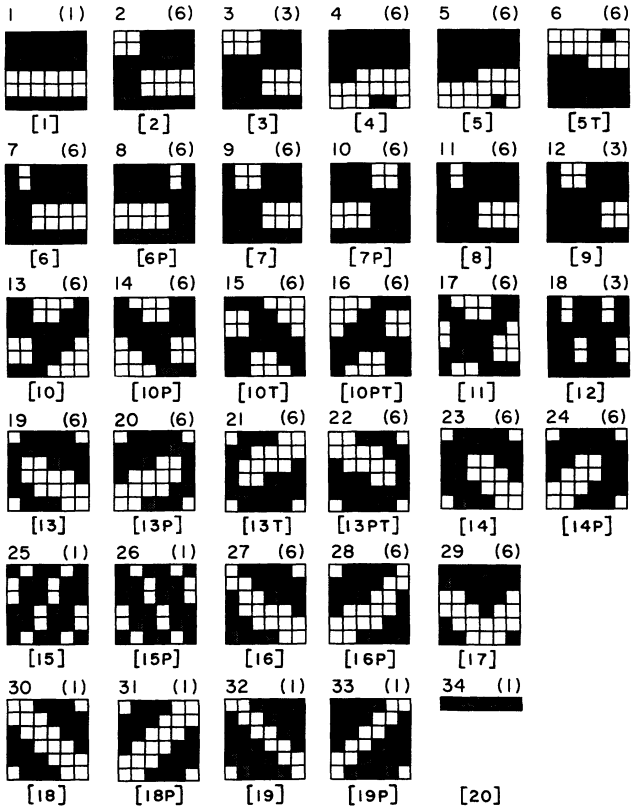

FIG. 4. The initial repertoire of MP's for a six-trion network with the connectivity given by Eq. (8) are found by following the most probable path in evolving all possible 3^{12} initial states according to Eq. (1) until repeating patterns, the MP's, are obtained. Each square represents a trion with three levels of firing activity as in Fig. 2. Each horizontal row represents a ring of interconnected (as in Fig. 2) trions (so that the sixth square wraps around to the first) and time evolves downward. There are a total of 155 MP's which can be completely classified by their distinct spatial rotations into 34 groups of MP's shown here. The group number is listed on the top left corner while the number of MP's in each group is given on the top right by ( ) (cyclically rotate the MP so that the first column is the second, etc.; if the MP is not a temporal rotation of any of the other elements in the group it is considered distinct). These 34 MP's are further classified, below each MP, into 20 symmetry groups [ ] according to the additional symmetries of parity P (reflection of trion number about a line separating two trions), time reversal T and a combination PT. An explicit example is shown in Fig. 5. In a Monte Carlo calculation these MP's would flow from one to another.

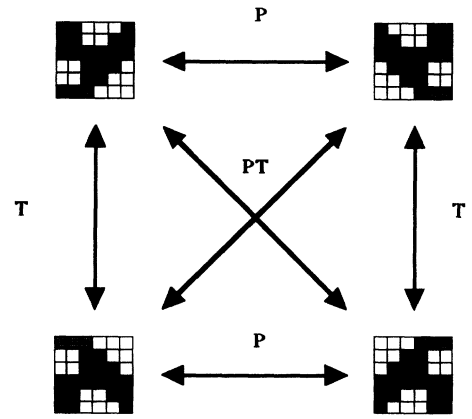

FIG. 5. An explicit example of the symmetry relations among the MP's in symmetry group [10] in Fig. 4.

There are 1804 MP's in the repertoire given by the connections [4]

$$V_{i,i+1}=V_{i,i-1}=1\ ,\quad W_{i,i+2}=W_{i,i-2}=-1\ , \tag{9}$$

thresholds $V_i=0$, all other V_{ij} equal to 0, $g(0)/g(\pm)=500$, $N=6$ trions, and $B>B(1)$ in Eq. (5). Using these symmetry operations R, P, T, and PT, in addition to an additional one, R_T rotating in space and time, present for these special sets of connections and numbers of trions, these 1804 MP's can be placed in 73 symmetry groups. This repertoire proved to be especially interesting when mapped onto music and onto robotic motion. An example of the MP's in two of these symmetry groups is given in Fig. 6. In one of these groups, the MP's with respect to spatial (and temporal) rotations have been arranged to make the symmetry relationships among the MP's more transparent. We leave it as an exercise for the reader to see these relationships among the complex spatial-temporal patterns in Fig. 6. This helps illustrate the power of these networks that can readily recognize these relationships as illustrated in the examples shown in Sec. V.

We suspect that there may be additional general symmetries to be discovered, especially when several columnar networks are coupled together. We suggest that these groups or categories of MP's defined by symmetry operations are not only useful in understanding aspects of pattern recognization such as rotational invariance, but will prove invaluable in understanding the nature of the sequences of transitions of the MP's among themselves. A relevant example of a MP evolving into other MP's in Monte Carlo evolutions is shown in Fig. 7.

We have called the above symmetries "global" in our columnar MP's, in contrast to "local" ones in which the temporal patterns for two specific trions might be interchanged (with a possible phase shift in time). For example, for the repertoire in Fig. 4, MP 2 is related to MP 1 by shifting the patterns for trions 1 and 2 by three time steps (or applying C to just these two trions). We note then that all the MP's in Fig. 4 consist "simply" of combinations of just three temporal patterns for individual trions:

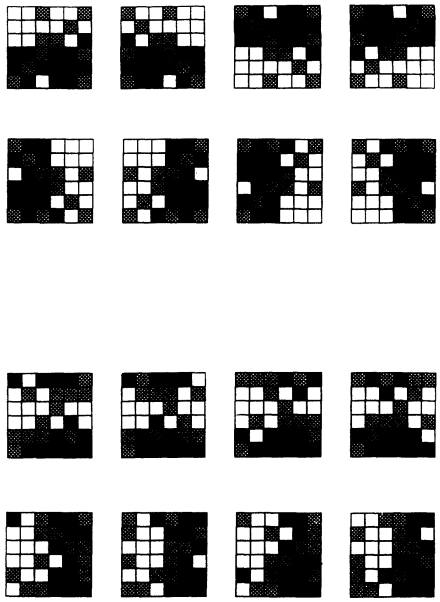

FIG. 6. Example of the MP's in two symmetry groups in the repertoire (see Figs. 4 and 5) for the connectivity (9). Each symmetry group consists of eight MP's related by combinations of P, T, and a symmetry operation specific to this repertoire corresponding to a spatial-temporal rotation of 90° about the center of the MP. In the first symmetry group, the MP's with respect to spatial (and temporal) rotations have been arranged to make the symmetry relationships among the MP's more transparent. We leave it as an exercise for the reader to see these relationships among these MP's. This exercise will help illustrate the power of these trion networks that can readily recognize these symmetry relationships (as illustrated in the examples shown in Sec. V).

$$\begin{aligned} a&=(+,+,0,-,-,0)\ ,\\ b&=(+,+,+,-,-,-)\ ,\\ c&=(0,0,0,0,0,0)\ . \end{aligned} \tag{10}$$

It would be of strong interest to analytically determine the repertoire starting from this "alphabet" (10). [Note that this alphabet (10) holds for the repertoire from the connectivity (8) with any number of trions >3.] We see from Table VI of [6] that for connectivity $V_{ii}=1$, $V_{i,i+1}=V_{i,i-1}=1$, $W_{ij}=-V_{ij}$, the repertoire has 246 MP's and the alphabet consists of (10) plus $d=(-,+,-,+,-,+)$, $f=(+,-,0,-,+,0)$, $g=(+,0,+,-,0,-)$, and $h=(+,0,0,-,0,0)$. We are thinking of these trion temporal firing patterns (dependent on the connectivity) as letters, the columnar MP's as words. The extension to a higher level architecture is discussed in Sec. VI.

IV. LEARNING A MP

Consider now learning a MP from Fig. 4 using the Hebb learning algorithm, Eq. (2). The example of learning MP 6(2) [where the (2) denotes the MP obtained from the MP 6 specifically shown in Fig. 4, by operating twice with spatial rotation operator R] is shown in Fig. 8 where

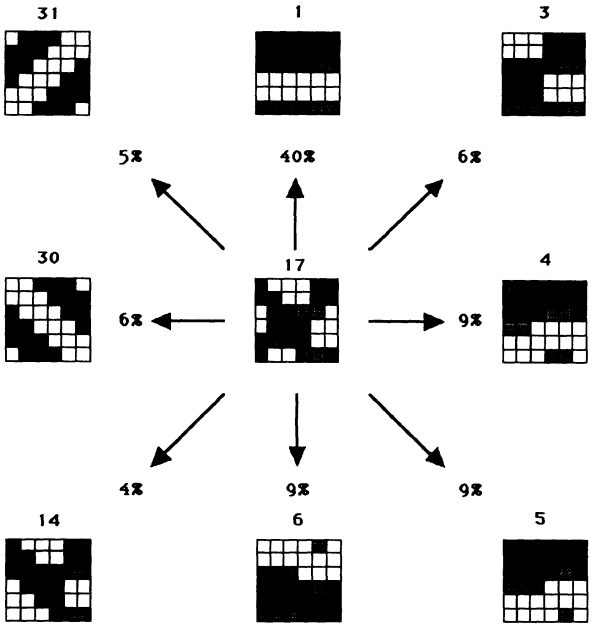

FIG. 7. Monte Carlo calculations for MP 17(0). The numbers at the end of the arrows give the percentage of 1000 Monte Carlo calculations that go to the eight other MP's (including all spatial rotations). Shown here are those MP's that are accessed with percentages greater than 3%. These relations can be substantially modified through learning.

we plot the probability of cycling P_C [as defined in Eq. (3)] versus ε. The B value 6.3 for this striking example of learning is particularly enhanced near this "transition" $B(1)$, see Eq. (5). Note as a result of learning this MP 6(2), the connections Eq. (8) will be modified according to Eq. (2). For example, here, $V_{5,6}=1$ and $V_{5,4}=1+2\varepsilon$, so that we say that the precise symmetry, $V_{i,i+1}=V_{i,i-1}=1$, is slightly broken by learning for small ε. This small symmetry breaking has been shown [13] to form the basis for a temporally rapid selectional learning in contrast to a much slower fine tuning of the parameters necessary for

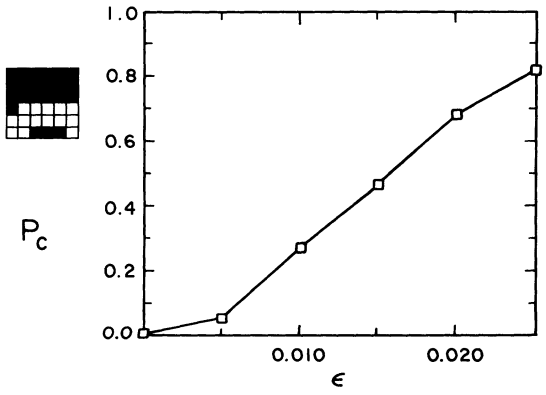

FIG. 8. The cycling probability, Eq. (3), P_C to remain in MP 6(2) [where (2) denotes a rotation of two trion sites from the MP 6 pictured in Fig. 4] versus the learning coefficient ε, Eq. (2) and $B=6.3$. This striking example of learning is particularly enhanced near the "transition" $B(1)$, Eq. (5).

instructional learning. (Both are probably necessary to understand behavior.) Below, we show that this symmetry breaking in the Hebb learning forms the basis for the recognition of the symmetries among the MP's present in a repertoire.

V. RECOGNITION OF ROTATIONAL INVARIANCE AND TIME REVERSAL

Here we discuss the recognition of spatially rotated and time-reversed objects in the trion model. This recognition of spatial rotational invariance is built into the highly structured trion model due to its natural symmetry relations Consider a simplified example in which a specific visual object is represented in the cortex by one of the MP's. Rotated VO's are represented by rotations of the MP of the standing VO. The VO seen in a normal standing position is learned with the Hebb rule and the symmetry among the connections is broken by a small amount. When a rotated VO is seen, the rotated VO MP evolves in a Monte Carlo calculation into the MP for the standing VO, thereby identifying it as a VO; the number of time steps to evolve is linearly related to the amount of rotation, in agreement with experiment [16]. A similar scenario is considered for recognition of time-reversed MP's. Here we do not give an explicit physical representation for the abstract MP's (although the mappings onto music [7,14] and robotic motion [21] are relevant). Examples are presented below.

Rotational invariance will be explored in the following example. Initially, when the subject sees an object, a MP will be selected out, e.g., MP 4(0) where the ( ) indicate the rotation of MP 4 in Fig. 4, so that 4(0) is the unrotated MP shown in Fig. 4. Before learning ($B=7.0$) this MP will then evolve into other MP's [see Fig. 7 for an example of the evolution of MP 17(0)].

If the network is presented with a rotated object then a rotated MP will be selected out [13]. Since the network has six trions each rotated MP corresponds to an angle of 30°, with MP 4(3) being a rotation of 90°. When the various rotated MP's were run in Monte Carlo calculations they evolved to MP 4(0) with a percentage inversely dependent on the rotation as shown in Fig. 9.

An example of one of the Monte Carlo calculations is shown below in Fig. 10 which started in MP 4(2) and evolved into MP 4(0) at the 26th time step, thereby taking 25 time steps to reach the learned MP or unrotated object. The Monte Carlo calculations were performed by searching for MP 4(0) within the first 50 time steps. This method was chosen so that evolutions that started in 4(2) went to 4(1) and then 4(0) would be counted. The percentage of runs going to MP 4(0) varied with the amount of rotation with those that are rotated more are less likely to reach the unrotated MP. These results are only for one column, and a realistic version would probably involve many columns. By "multiplexing" the input to a number of columns [22] or using interconnected columns [23] the performance can be improved.

The rotational invariance is examined for various values of ε, which may be the result of learning the unrotated object more on a single trial or having multiple tri-

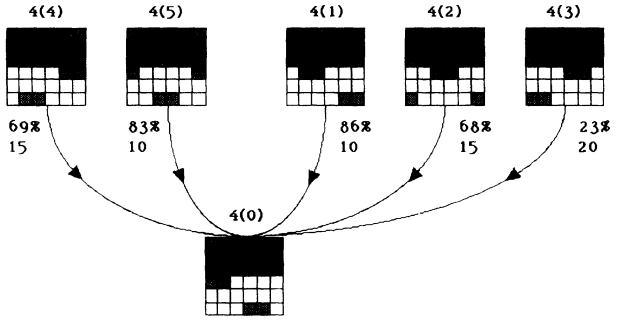

FIG. 9. Example of recognition of rotation invariance. Monte Carlo (1000 runs for 50 time steps) results from starting in each of the five rotated MP's [and then searching for MP 4(0) within the 50 time steps] after learning MP 4(0) with an $\varepsilon=0.025$ at $B=7.0$. Both the percentage of runs evolving to MP 4(0) and the average number of time steps taken $\langle t \rangle$ are shown.

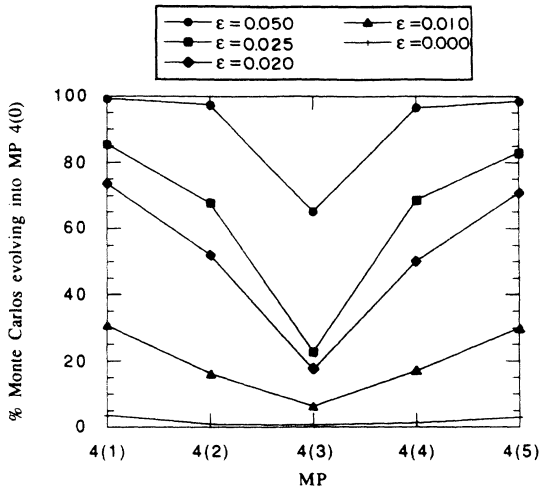

FIG. 11. The percentage (%) of Monte Carlo calculations (Fig. 9) for the rotated MP's that evolve into MP 4(0) within the first 50 time steps for various values of ε. Recall that MP's 4(1) and 4(5) are closest in rotation to 4(0), whereas 4(3) is furthest away. (The straight lines are for visual guidance.)

als which keep increasing ε in increments. The percentage of Monte Carlos (Fig. 11) that evolve into MP 4(0) are improved for all rotations and are starting to saturate for $\varepsilon=0.05$, which would be considered a large learning coefficient. The rotation is symmetric for clockwise and counterclockwise rotations.

The average number of time steps $\langle t \rangle$ for the Monte Carlo calculations to reach MP 4(0) is shown in Fig. 12. Notice that the $\langle t \rangle$ is also symmetric, being the same for both clockwise and counterclockwise rotations. Also, the $\langle t \rangle$ is linear with the angle of rotation since each rotated MP is an additional rotation of 30°. The two time step next-nearest neighbor learning rule was used in this example (see [14,15] for use of the three time step next-nearest neighbor learning rule, as well as a discussion [15] of allowing one or two errors in the recall).

In addition to being able to identify rotations the network can also identify a time-reversal operation. Besides the rotational symmetries for group 6, the time reversal T yield distinct MP's forming their own rotational group 5, so that MP 6(2) is transformed into MP 5(2). The rotation groups for MP 5 and MP 6 are related through a time-reversal operation T as shown in Fig. 4. The Monte Carlo evolution results identifying both rotations and time reversal after learning MP 6(2 with an $\varepsilon=0.025$ for two time steps at $B=7.0$ are shown in Fig. 13.

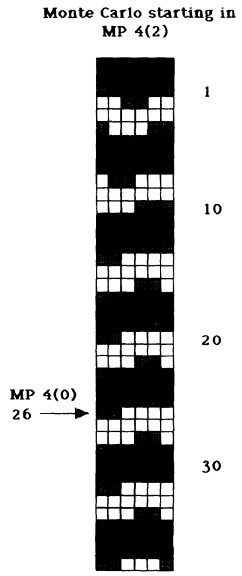

FIG. 10. A Monte Carlo calculation (Fig. 9) starting in MP 4(2). The evolution reaches the learned MP 4(0) at the 26th time step.

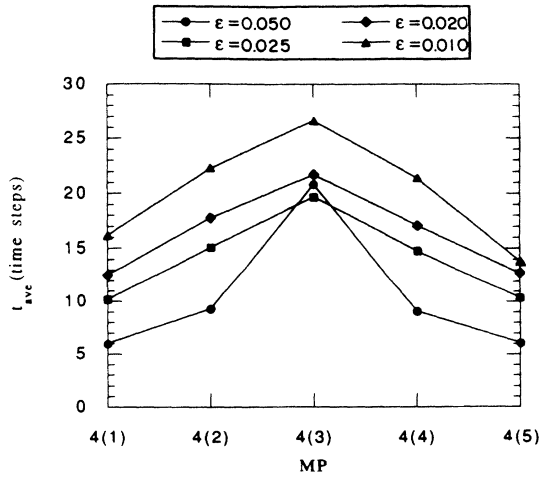

FIG. 12. The average number of time steps $\langle t \rangle$ for the Monte Carlo calculations (Fig. 9) for the rotated MP's that evolve into MP 4(0) within the first 50 time steps for various values of ε.

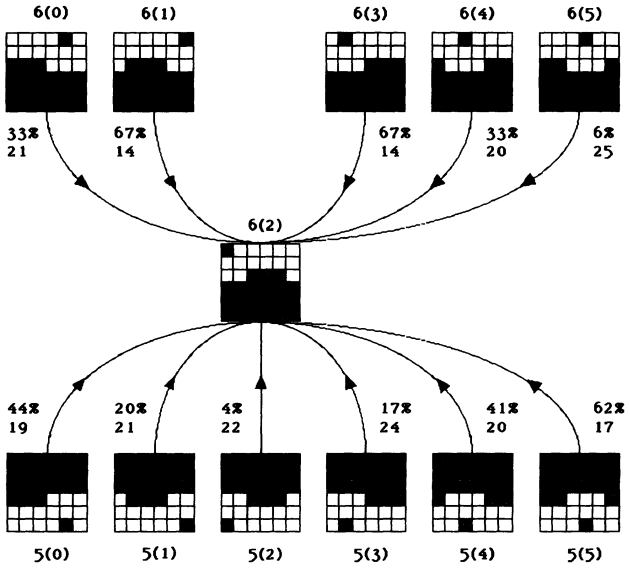

FIG. 13. Example of both rotation and time-reversal recognition in Monte Carlo calculations (see Fig. 9) after learning MP 6(2). MP's 5 are related to MP's 6 by T.

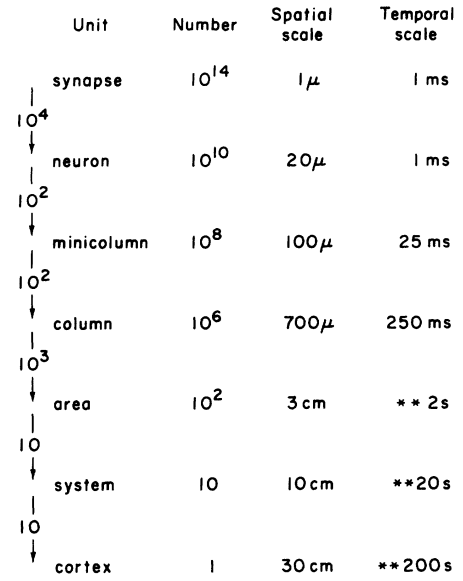

FIG. 14. Very rough spatial and temporal scales for various structures, along with their number, in cortex. The numbers on the left between structures represent the number of units of the structure above in the structure below, e.g., there are roughly 10^2 neurons in a minicolumn. The spatial scales for minicolumn and larger should be considered perpendicular to the cortical surface after it is unfolded and flattened out. We consider the spatial and temporal scales of 100 μm and 25 ms and larger, respectively, as those which we explicitly consider here. The three temporal scales marked with ** are proposed new scales [6] and may be related to all the spatial scales of column and larger.

VI. DISCUSSION

We have proposed in this paper that symmetry operations are a crucial feature of higher brain function and result from the spatial and temporal modularity of the cortex. It is interesting to stress the general role of pattern development in biological systems. Waddington [24] in referring to growth of various animals states "the dominant characteristic of biological proportions is that any given form usually exhibits the simultaneous operation of several rules of proportion, rather than of only one. And in discussing these proportions, it becomes extremely superficial to omit the time factor, since in the great majority of instances the proportions of a biological form change as it grows and develops." This fits in nicely with our ideas of pattern development in the brain [25] as shown in the evolution of the trion model spatial-temporal firing patterns and the symmetry relations among these patterns as they evolve dynamically. As shown in Fig. 14, there are many spatial and temporal scales in the cortex. Only those spatial scales for the minicolumn and larger, and temporal scales of 25 ms and longer, are considered here. The symmetry operations arise naturally in the highly structured trion model of the cortex. A columnar network of a small number of trions has a large repertoire of quasistable, periodic spatial-temporal firing patterns, MP's, which an be excited. The MP's are related by specific symmetries: spatial rotation, parity, "spin" reversal, and time reversal as well as other "global" symmetry operations in this abstract internal language of the brain. These MP's can be readily enhanced (as well as inherent categories of MP's) by only a small change in connection strengths via a Hebb learning rule. Learning introduces small breaking of the symmetries in the connectivities which enables a symmetry in the patterns to be recognized in the Monte Carlo evolution of the MP's: We presented, in Sec. V, detailed examples of the recognition of rotational invariance and of a time-reversed pattern via this procedure.

As shown in Fig. 1, the cortical columns may themselves be organized in a very highly structured manner to form a cortical area: It is this higher level architecture that must be examined in order to explore the further consequences of the concepts concerning computation by symmetry operations introduced in this paper. Clearly any analytic insight into the behavior of this architecture would be extremely useful. We suggest that a hardware analog-digital implementation of this higher level cortical area architecture of trion cortical columns shown in Fig. 1 should be "straightforward" due to the localized and structured (in space and time) connectivity, and the discreteness of the firing levels. (A more "biological" version could also be considered in which these discrete quantities are allowed some spread in order to optimize the "behavior" of the model.) The high speed parallel computations will allow us to look for symmetry operations in a cortical area.

We note the structured connectivity that permits the notation of the minicolumn, column, and cortical area, to be called functional cooperative units in a dynamical processing sense: the heavy interconnections vertically (excitatory and inhibitory) among the neurons through the cortical layers form the basis for the minicolumn; the (neurons in the) minicolumns are connected to neighboring minicolumns in the same column through horizontal

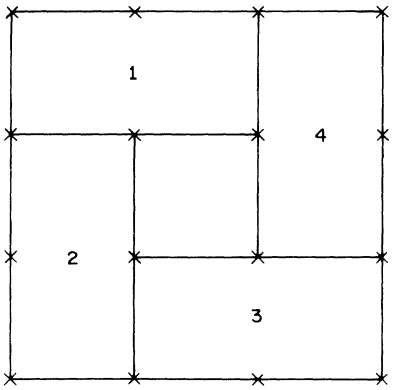

FIG. 15. Four coupled six-trion columnar networks labeled 1–4 are mapped onto a 4×4 Go board (with the 16 vertices labeled by ×) illustrating the chunking of the board into groups of six vertices and the overlap of the columnar networks onto some of the vertices.

connections in a weaker manner; the long-range connections between distant columns [26] are still highly specific and yet still weaker in strength. Thus it seems quite reasonable to think of (at least) three spatial scales of cooperativity defining the functional units of minicolumn, column, and cortical area. We note that "global" MP's [23] in the higher level architecture of coupled columnar trion networks, which follow from the nature of weak intercolumnar connectivity between minicolumns, are (primarily) products of the MP's from the individual columns (with specific temporal phase relations now being important).

We suggest that the computations by symmetry operation discussed here are involved in higher brain function. We have shown that simple mappings of the Monte Carlo evolutions of the trion model onto pitches and instruments produces recognizable human styles of music [7,14] and that the mappings onto robotic motion [21] give very interesting behavior. We now propose that a potential goal of a cortical area architecture is, by very "clever" mapping of these firing patterns onto a logic problem, to build a logic device. For example, insight into the solution of some simple "board" game would be a major advance toward building a thinking computer.

Some simple thoughts toward such a project of building a logic device to solve board games can be mentioned: Insights gained from analysis of chess [27] show that master chess players recall a middle game position takes place through the use of "local clusters of pieces." As noted by Chase and Simon [27], the master's strategy in choosing a next move in a middle game is very interesting: "As we have shown, the board is organized into smaller units representing more local clusters of pieces. Since some of these patterns have plausible moves associated with them in long-term memory, the master will start his search by taking one of these moves and analyzing its consequences. Since some of the recognizable patterns will be relevant, and some irrelevant, to his analysis, we hypothesize that he constructs a more concrete internal representation of the relevant patterns in the mind's eye, and then modifies these patterns to reflect the consequences of making the evoked move. The information processes needed . . . are akin to the rotation processes when the internal representation of the position is updated the result is then passed back through the pattern perception system and new patterns are perceived. These patterns in turn will suggest new moves and the search continues." It is well known that the organization of the visual information in the cortex is such that the receptive fields overlap in neighboring columns.

We illustrate these two features of chunking or use of local clusters and of overlap in information in the simple example of a 4×4 Go game shown in Fig. 15: four coupled six-trion columnar networks labeled 1–4 are mapped onto a 4×4 Go board illustrating the chunking of the board into groups of six vertices and the overlap of the columnar networks onto some of the vertices. We have in mind mapping a few winning strategies of play in this 4×4 Go game onto trion model evolutions and enhancing these evolutions using the Hebb rule in a selective and very rapid manner [13] for the coupled networks [23]. The goal would be to see if these winning strategies generalized to other moves. Clearly, achieving this goal for any nontrivial board game will be a challenge, but of considerable significance.

ACKNOWLEDGMENTS

We thank Minko Balkanski, Mark Bodner, David Kirkman, Carver Mead, Jiri Patera, and Edward Thorp for helpful discussions. This research was supported in part by the REU program of the National Science Foundation and by the National Association of Music Merchants. K.S. was supported in part by the University of California.

[1] H. Weyl, *Symmetry* (Princeton, Princeton, NJ, 1952); *Module Proportion, Symmetry, Rhythm,* edited by G. Kepes (Braziller, New York, 1966); D. Eisenberg and D. Crothers, *Physical Chemistry with Applications to Life Sciences* (Benjamin/Cummings, Menlo Park, 1979).

[2] D. H. Hubel and T. N. Wiesel, Proc. R. Soc. London, Ser. B **198**, 1 (1977); P. S. Goldman and W. H. J. Nauta, Brain Research **122**, 393 (1977); P. S. Goldman-Rakic, Trends Neurosci. **7**, 419 (1984); G. L. Shaw, E. Harth, and A. B. Scheibel, Exp. Neurol. **77**, 324 (1982); G. C. Blasdel and G. Salama, Nature (London) **321**, 579 (1986); T. Bonhoeffer and A. Grinvald, *ibid.* **353**, 429 (1991); C. M. Gray and P. Konig, A. K. Engel, and W. Singer, *ibid.* **338**, 334 (1989); C. M. Gray and W. Singer, Proc. Natl. Acad. Sci. USA **86**, 1698 (1989); W. Singer, Concepts Neurosci. **1**, 1 (1990); R. Eckhorn, R. Bauer, W. Jordan, M. Brosch, W. Kruse, and H. J. Reitboeck, Biol. Cybern. **6**, 121 (1988); H. R. Dinse, K. Kruger, and J. Best, Concepts Neurosci. **1**, 199 (1990); G. L. Shaw, J. Kruger, D. J. Silverman, AM. H. J. Aersten, F. Aiple, and H. C. Liu, Neurol. Res. **15**, 46 (1993).

[3] D. O. Hebb, *Organization of Behavior* (Wiley, New York,

1949).
[4] G. L. Shaw, D. J. Silverman, and J. C. Pearson, Proc. Natl. Acad. Sci. USA **82**, 2364 (1985).
[5] D. J. Silverman, G. L. Shaw, and J. C. Pearson, Biol. Cybern. **53**, 259 (1986).
[6] J. V. McGrann, G. L. Shaw, D. J. Silverman, and J. C. Pearson, Phys. Rev. A **43**, 5678 (1991).
[7] X. Leng, G. L. Shaw, and E. L. Wright, Music Percept. **8**, 49 (1990); X. Leng and G. L. Shaw, Concepts Neurosci. **2**, 229 (1991).
[8] V. B. Mountcastle, in *The Mindful Brai,* edited by G. M. Edelman and V. B. Mountcastle (MIT, Cambridge, MA, 1978), p. 1.
[9] W. von Seelen, Kybernetik **7**, 89 (1970); V. Braitenberg and C. Braitenberg, Biol. Cybern. **33**, 179 (1979).
[10] L. Brothers, G. L. Shaw, and E. L. Wright, Neurol. Res. **15**, 413 (1993); L. Brothers and G. L. Shaw, in *Models of Brain Function,* edited by R. Cotterill (Cambridge University, Cambridge, England, 1989).
[11] W. A. Little, Math. Biosci. **19**, 101 (1974); Concepts Neurosci. **1**, 149 (1990).
[12] M. E. Fisher and W. Selke, Phys. Rev. Lett. **44**, 1502 (1980).
[13] K. V. Shenoy, J. Kaufman, J. . McGrann, and G. L. Shaw, Cerebral Cortex **3**, 239 (1993).
[14] X. Leng, Ph.D. thesis, University of California, Irvine, 1990.
[15] J. V. McGrann, Ph.D. thesis, University of California, Irvine, 1992.
[16] L. A. Cooper and R. N. Shepard, in *Visual Information Processing,* edited by W. G. Chase (Academic, New York, 1973), p. 75; R. N. Shepard and J. Metzler, Science **171**, 70 1 (1971).
[17] For previous neural network approaches, see, e.g., V. S. Dotsenko, J. Phys. A **21**, L783 (1988); C. von der Malsburg and E. Bienenstock, Europhys. Lett. **3**, 1243 (1987); R. Kree and A. Zippelius, J. PHys. A **21**, L813 (1988). In general, the desired symmetries are explicitly introduced.
[18] K. J. Roney and G. L. Shaw, Math. Biosci. **51**, 25 (1980); G. L. Shaw and K. J. Roney, Phys. Lett. **74A**, 146 (1979).
[19] G. L. Shaw and R. Vasudean, Math. Biosci. **21**, 207 (1974).
[20] B. Katz, *The Release of Neural Transmitter Substances* (Thomas, Springfield, IL, 1969).
[21] S. J. Shanbhag and G. L. Shaw (unpublished).
[22] J. von Neumann, in *Automata Studies,* edited by C. E. Shannon and J. McCarthy (Princeton University, Princeton, NJ, 1956).
[23] J. A. Quillfeldt, M. Sardesai, and G. Shaw (unpublished); Fig. 16 of X. Leng, J. V. McGrann, J. A. Quillfeldt, G. L. Shaw, and K. V. Shenoy, in *Neural Bases of Learning and Memory,* edited by J. Delacour (World Scientific, Singapore, in press).
[24] C. H. Waddington, in *Module, Proportion Symmetry, Rhythm,* edited by G. Kepes (Braziller, New York, 1966), p. 20.
[25] For another approach to symmetries in spatial-temporal adaptive evolution of finite systems, see J. Patera, G. L. Shaw, R. Slansky, and X. Leng, Phys. Rev. A **40**, 1073 (1989).
[26] We note the structured long-range connectivity between neurons and groups of neurons: Fig. 12a of C. D. Gilbert and T. N. Wiesel, J. Neurosci. **3**, 1116 (1983), which shows a clustering of synapses at spacings of 90 μm. Gilbert and collaborators [C. D. Gilbert and T. N. Wiesel, J. Neurosci. **9**, 2432 91989); J. A. Hirsch and C. D. Gilbert, *ibid.* **11**, 1800 (1991)] have shown long-ranged lateral axons connecting columns in primary visual cortex up to 8 mm apart via neurons in minicolumns having the same orientation "specificity." K. S. Rockland and A. Virga, J. Comp. Neurol. **285**, 54 (1989) have shown the very structured connectivity projecting back from secondary to primary visual cortex in macaque. Other results [Goldman-Rakic, [2]; K. S. Rockland, Visual Neurosci. **3**, 155 (1989)] show connectivity from one cortical area to another over large distances is via specific (columnar) patches.
[27] See the relevant discussion of chess strategies in W. S. Boettcher, S. S. Hahn, and G. L. Shaw, Leonardo Music J. (to be published), as summarized from W. G. Chase and H. A. Simon, in *Visual Information Processing,* edited by W. G. Chase (Academic, New York, 1973), p. 215; and A. de Groot, *Thought and Choice in Chess* (Mouton, The Hague, 1965).

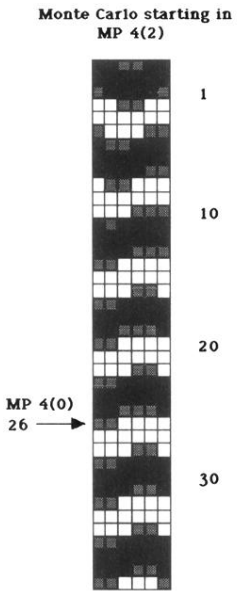

FIG. 10. A Monte Carlo calculation (Fig. 9) starting in MP 4(2). The evolution reaches the learned MP 4(0) at the 26th time step.

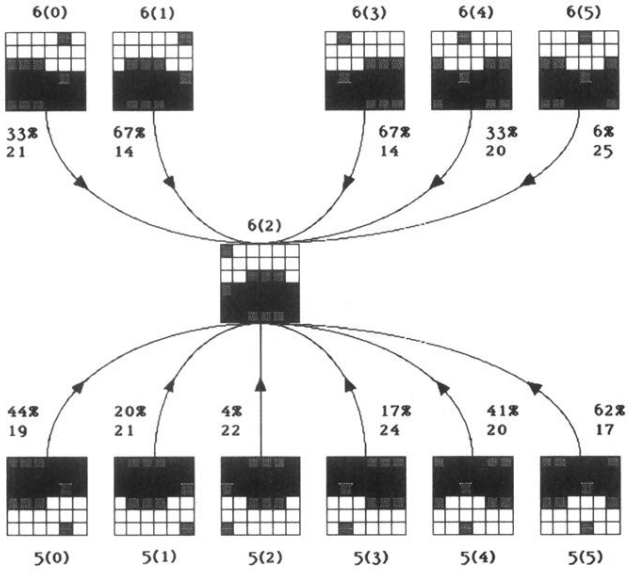

FIG. 13. Example of both rotation and time-reversal recognition in Monte Carlo calculations (see Fig. 9) after learning MP 6(2). MP's 5 are related to MP's 6 by T.

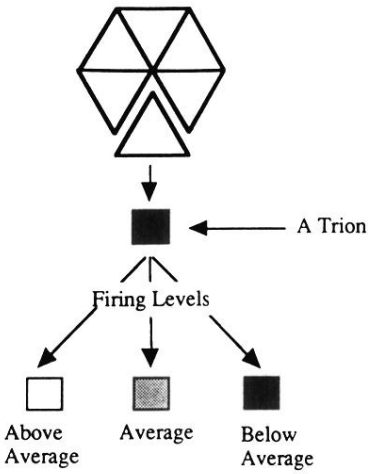

FIG. 2. We identify a minicolumn with the idealized trion and the basic network of trions is the cortical column. As shown, the trion has three levels of firing activity.

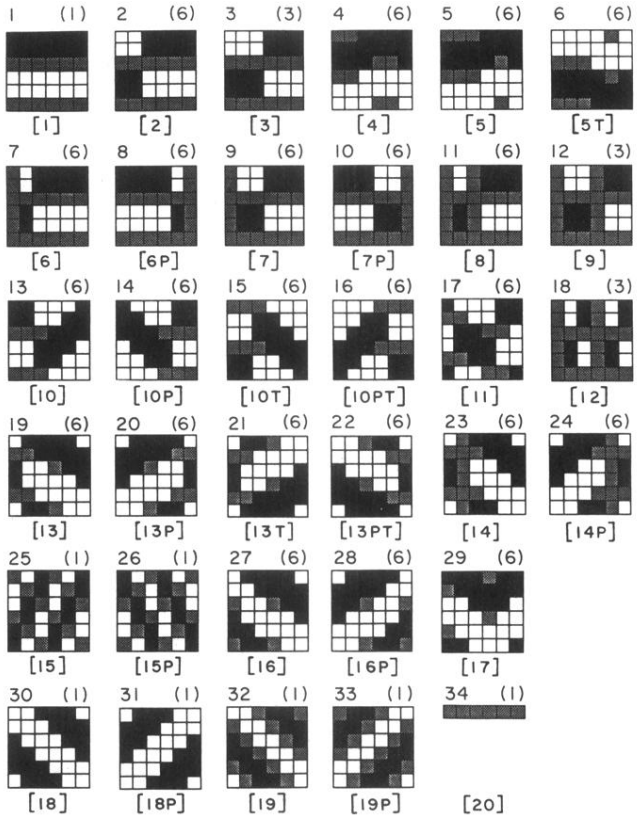

FIG. 4. The initial repertoire of MP's for a six-trion network with the connectivity given by Eq. (8) are found by following the most probable path in evolving all possible 3^{12} initial states according to Eq. (1) until repeating patterns, the MP's, are obtained. Each square represents a trion with three levels of firing activity as in Fig. 2. Each horizontal row represents a ring of interconnected (as in Fig. 2) trions (so that the sixth square wraps around to the first) and time evolves downward. There are a total of 155 MP's which can be completely classified by their distinct spatial rotations into 34 groups of MP's shown here. The group number is listed on the top left corner while the number of MP's in each group is given on the top right by ( ) (cyclically rotate the MP so that the first column is the second, etc.; if the MP is not a temporal rotation of any of the other elements in the group it is considered distinct). These 34 MP's are further classified, below each MP, into 20 symmetry groups [ ] according to the additional symmetries of parity P (reflection of trion number about a line separating two trions), time reversal T and a combination PT. An explicit example is shown in Fig. 5. In a Monte Carlo calculation these MP's would flow from one to another.

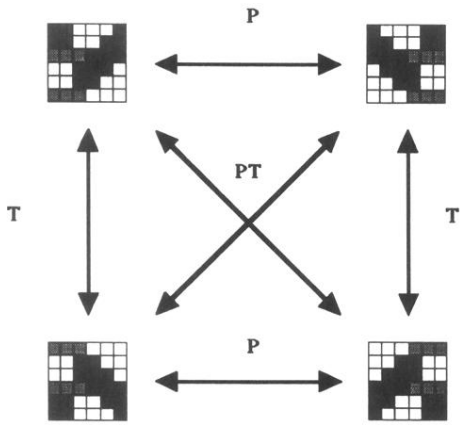

FIG. 5. An explicit example of the symmetry relations among the MP's in symmetry group [10] in Fig. 4.

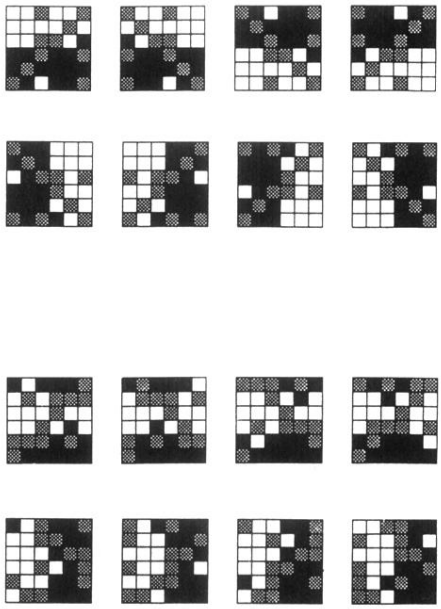

FIG. 6. Example of the MP's in two symmetry groups in the repertoire (see Figs. 4 and 5) for the connectivity (9). Each symmetry group consists of eight MP's related by combinations of P, T, and a symmetry operation specific to this repertoire corresponding to a spatial-temporal rotation of 90° about the center of the MP. In the first symmetry group, the MP's with respect to spatial (and temporal) rotations have been arranged to make the symmetry relationships among the MP's more transparent. We leave it as an exercise for the reader to see these relationships among these MP's. This exercise will help illustrate the power of these trion networks that can readily recognize these symmetry relationships (as illustrated in the examples shown in Sec. V).

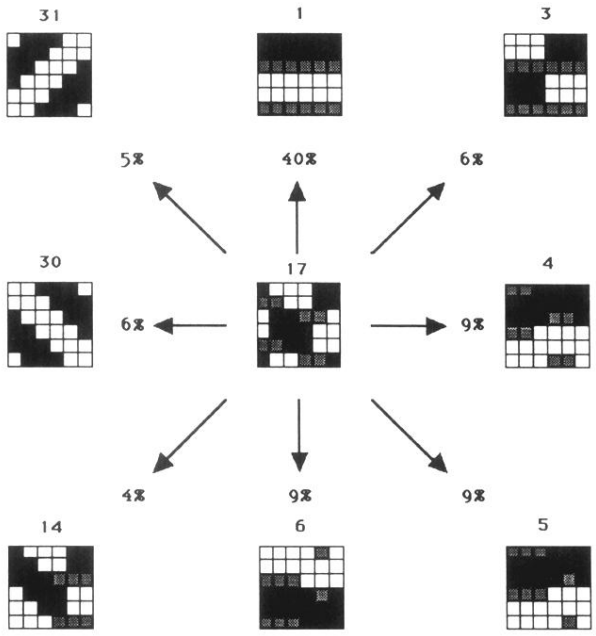

FIG. 7. Monte Carlo calculations for MP 17(0). The numbers at the end of the arrows give the percentage of 1000 Monte Carlo calculations that go to the eight other MP's (including all spatial rotations). Shown here are those MP's that are accessed with percentages greater than 3%. These relations can be substantially modified through learning.

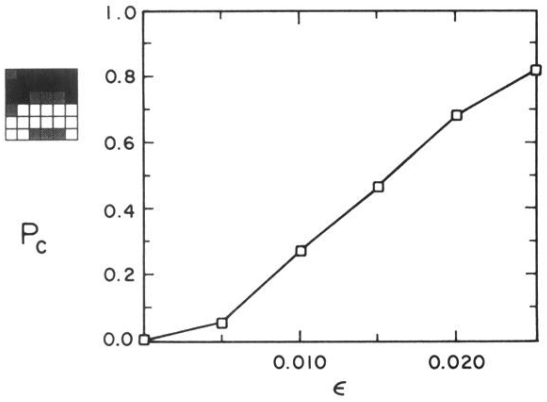

FIG. 8. The cycling probability, Eq. (3), P_C to remain in MP 6(2) [where (2) denotes a rotation of two trion sites from the MP 6 pictured in Fig. 4] versus the learning coefficient ε, Eq. (2) and $B = 6.3$. This striking example of learning is particularly enhanced near the "transition" $B(1)$, Eq. (5).

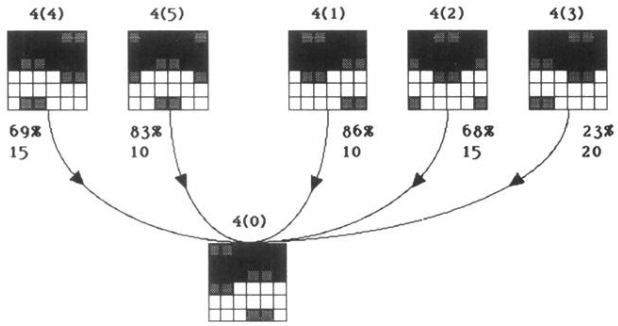

FIG. 9. Example of recognition of rotation invariance. Monte Carlo (1000 runs for 50 time steps) results from starting in each of the five rotated MP's [and then searching for MP 4(0) within the 50 time steps] after learning MP 4(0) with an $\varepsilon=0.025$ at $B=7.0$. Both the percentage of runs evolving to MP 4(0) and the average number of time steps taken $\langle t \rangle$ are shown.